Engineering Geology 228 (2017) 97–106

Contents lists available at ScienceDirect

Engineering Geology

journal homepage: www.elsevier.com/locate/enggeo

Spatial modeling of discontinuity intensity from borehole observations at El Teniente mine, Chile

Amin Hekmatnejad[a,b], Xavier Emery[a,b,*], Andrés Brzovic[c,d], Paulina Schachter[c], Javier A. Vallejos[a,b]

[a] Department of Mining Engineering, University of Chile, Santiago, Chile
[b] Advanced Mining Technology Center, University of Chile, Santiago, Chile
[c] Codelco Chile, El Teniente Division, Rancagua, Chile
[d] Institute of Engineering Sciences, University of O'Higgins, Rancagua, Chile

ARTICLE INFO

Keywords:
Discontinuity area per unit volume
Terzaghi correction
Geostatistical simulation
Spatial uncertainty
Spatial interpolation
Weak veins

ABSTRACT

This work addresses the problem of predicting the discontinuity intensity P_{32} (discontinuity area per unit volume of rock mass) in space and of quantifying the uncertainty in the true P_{32} values, using information from observed discontinuities intersecting boreholes. This problem is relevant in various fields of engineering, including mining applications, hydrocarbon extraction, groundwater modeling and civil works. The main idea is to calculate experimental P_{32} values for borehole segments (composites), based on a Terzaghi weighting of the discontinuities that intersect the boreholes. A validation exercise performed on simulated discrete fracture networks demonstrates that the calculated P_{32} values provide unbiased predictions of the true P_{32}, at both global and local scales, and can therefore be used as experimental data for spatial interpolation purposes.

By using geostatistical simulation techniques, the spatial prediction of the P_{32} and the corresponding measures of uncertainty can be obtained on a block-by-block basis. This methodology is applied to a data set from the El Teniente copper mine, Codelco-Chile. The objective is to map the expected values of the intensity of stockwork veins with a weak infill mineral assemblage and a typical thickness greater than 1 mm, which are referred to as weak veins. Confidence limits on this intensity and its probability of exceeding given critical values are also estimated. The quality of the prediction and of the uncertainty quantification is checked by leave-one-out cross-validation. The resulting confidence limits and probability maps can be used as indicators to define geotechnical domains in the rock mass.

1. Introduction

The necessity of modeling discontinuities in rock masses has led to the use of Discrete Fracture Networks (DFN) as an important tool in rock mechanics for mining applications, hydrocarbon extraction, groundwater modeling and civil works design. To this end, an important task is the three-dimensional (3D) characterization of discontinuity properties, which include the number of discontinuity sets and, for each set, the number, orientation, spacing, location, shape and size of the discontinuities. Such a characterization relies on three main types of survey: borehole (1D), scanline and areal (2D) surveys, which can be complemented by analog surveys and 3D information obtained through remote sensing (Sturzenegger et al., 2011; Riquelme et al., 2015; Tuckey and Stead, 2016). In borehole surveys, the measurements are made on cores and oriented cores, or are deduced from petrophysical logs. For each observed discontinuity, its location, orientation, infill (type and thickness), aperture, surface geometry, etc., are noted. The information provided by borehole measurements is the distribution of the discontinuity orientation, the discontinuity density and the presence of discontinuity clusters, whereas 2D surveys allow evaluating the discontinuity size distribution, which is an essential parameter in the study of the mechanical and hydraulic properties of rock masses.

The discontinuity intensity, denoted as P_{32} and defined as the mean area of discontinuities per unit volume of rock mass, is one of the preferred ways for describing the degree of fracturing of a rock mass, as it is an additive and non-directional parameter. Dershowitz and Herda (1992) derive P_{32} by using proportionality relationships with the 1D discontinuity frequency (P_{10}) observed in boreholes or scanline surveys, or with the 2D discontinuity frequency (P_{21}) observed in areal surveys

* Corresponding author at: Department of Mining Engineering, University of Chile, Santiago, Chile.
E-mail addresses: amin.hekmatnejad@ing.uchile.cl (A. Hekmatnejad), xemery@ing.uchile.cl (X. Emery), ABrzovic@codelco.cl (A. Brzovic), pschacht@codelco.cl (P. Schachter), javallej@ing.uchile.cl (J.A. Vallejos).

http://dx.doi.org/10.1016/j.enggeo.2017.07.012
Received 11 January 2017; Received in revised form 27 June 2017; Accepted 31 July 2017
Available online 02 August 2017
0013-7952/

such as outcrops. However, both P_{10} and P_{21}, as well as the proportionality factors used to convert them into P_{32}, are non-additive, directional and subject to sampling biases. These features make them difficult to model and predict in space. For their part, Zhang and Einstein (2000) propose to separately estimate the total number of discontinuities and their size distribution, using data from different sources (borehole and areal surveys) and assuming that the discontinuities are disc-shaped and that the spatial distribution of their centers is a Poisson point process. The latter assumption corresponds to the idea of discontinuity centers uniformly distributed over space, which may actually not agree with reality. The previous approaches are further criticized by Chilès et al. (2008), who advocate a direct prediction of the discontinuity intensity from borehole data, accounting for the angles at which the borehole intersects the discontinuities, which avoids estimating the number, frequency and size of the discontinuities. In many situations these parameters are associated with a large uncertainty, whereas the discontinuity intensity P_{32} can be predicted directly with more robustness (Chilès et al., 2008).

In this paper, it is of interest to locally predict the discontinuity intensity from a set of borehole data and to quantify the uncertainty associated with the true (unknown) values of discontinuity intensity. In Section 2, a methodology for the prediction of the discontinuity intensity P_{32}, based on the former work of Chilès et al. (2008), is presented. Section 3 is aimed at applying this methodology to a real data set from El Teniente copper mine, Central Chile, in order to locally predict the veinlet intensity and to quantify its uncertainty at unsampled locations, by means of geostatistical simulation techniques. In recent years, it has been observed that rock structure is an important control factor for the large geomechanical instabilities in the El Teniente mine (rock bursts) and, in many cases, structures that define the over break correspond to geological discontinuities (veinlets) that are sub parallel to the excavations (Gonzalez and Brzovic, 2015). All this motivates the modeling of these geological discontinuities for investigating all aspects of the mining operation, like fragmentation, cave ability and safety while excavating in El Teniente mine.

2. Methodology: direct calculation of P_{32} on borehole composites

2.1. Principle

The methodology used in this work consists in converting the information of a normal borehole (with a diameter of about 10 cm) directly into P_{32} values for a certain length L of composites (i.e., segments of the borehole that participated in data surveying). It is based on the method proposed by Chilès et al. (2008), in which the i-th discontinuity intersecting a borehole composite with length L is weighted by the inverse of the cosine of the acute angle between the borehole direction (α) and the direction of the unit vector perpendicular to the surface of the discontinuity (ω_i), in agreement with the Terzaghi correction (Terzaghi, 1965):

$$\hat{P}_{32} = \frac{1}{L}\sum_{i=1}^{N}\frac{1}{|\cos(\omega_i - \alpha)|} \quad (1)$$

where N stands for the total number of discontinuities that intersect the borehole composite. In practice, one should make some modifications in the case when a discontinuity is sub-parallel to the borehole, to which the Terzaghi correction gives a very large weight (even infinite in the case of a parallel discontinuity). Some authors (Yow, 1987; Chilès et al., 2008) suggest a lower limit of 10 to 15° as the minimum allowed acute angle and replace all the smaller acute angles by this limit, which improves the robustness of the estimator in Eq. (1). The composite length L can be freely chosen by the practitioner: larger lengths will provide data with a smaller resolution, but with less dispersed P_{32} values, due to the so-called support effect (Chilès and Delfiner, 2012).

2.2. Validation on a synthetic case study

To validate the previous methodology, the proposed estimator of P_{32} is now applied to simulated fracture networks for which the true P_{32} values can be calculated, either globally or locally. For each simulation, a sampling mesh (for simplicity, with vertical boreholes) is considered and the experimental value of P_{32} is calculated for composites with a given length L using Eq. (1). The true and experimental values are then compared to check unbiasedness.

2.2.1. Steps of the study

Specifically, the steps of the experiment are the following.

(1) Step 1: Simulation of a discrete fracture network (DFN) corresponding to a 3D Poisson Boolean model of random discs (Chilès and Delfiner, 2012). For this purpose, one first simulates a Poisson point process with an intensity λ that indicates the average number of points per unit volume. Then, a discontinuity is assigned to each point, which corresponds to a disc with a random orientation and a random diameter, independent from the discs assigned at the other points of the Poisson process.
(2) Step 2: Calculation of the true discontinuity intensity for a given parallelepiped block, which relies on the calculation of the area of the intersection of a circular discontinuity with the block. To this end, the intersection between the discontinuity plane and the block is determined first. Such an intersection can be empty, a single point or a line segment (if the plane is tangent to the block) or a polygon with three to six vertices. In the former three cases, the intersection area is zero, so only the case of a polygonal intersection remains to be considered (Fig. 1A). The vertices of the polygon that are located outside the discontinuity (i.e., the vertices distant more than the discontinuity radius from the discontinuity center) are removed and replaced by the vertices corresponding to the intersection of the polygon with the discontinuity circumference (Fig. 1B). Finally, the area of the intersection between the discontinuity and the block is obtained as the sum of triangle and circular segment areas (Fig. 1C).
(3) Step 3: Calculation of the experimental discontinuity intensity for borehole samples using Eq. (1).
(4) Step 4: Comparison of the experimental and true values of the discontinuity intensity obtained at steps (2) and (3). The comparison is held globally, considering a parallelepiped block equal to the whole region of interest, and locally, considering smaller blocks.

The previous steps are repeated for 500 independent simulations of the discontinuity network based on the following parameters (Fig. 2):

- The region of interest is a cube with size 300 m × 300 m × 300 m.
- For the local study, the region is divided into cubic sub-blocks with size 60 m × 60 m × 60 m.
- The sampling mesh is 60 m along the north-south and east-west directions, so that one borehole is located at the center of each sub-block. The experimental discontinuity intensity is calculated on a composite of 60 m, in order to have one estimate ($\hat{P}_{32}$) for each sub-block and to compare it with the actual P_{32} value of this sub-block.
- The discontinuity diameters have a lognormal distribution truncated to a maximum discontinuity diameter of 20 m.
- The intensity of the Poisson point process is set to $\lambda = 0.03$. This implies an average number of 983,040 discontinuities that are likely to intersect the region of interest.
- A Fisher distribution with a mean pole direction of azimuth 60° and dip 30° and a Fisher concentration parameter κ equal to 25 (Fisher, 1953) is considered for the orientation of the discontinuity poles, in order to mimic realistic geological conditions. The Fisher concentration parameter describes the dispersion of an orientation cluster. A large κ value implies a tighter cluster, while a small κ

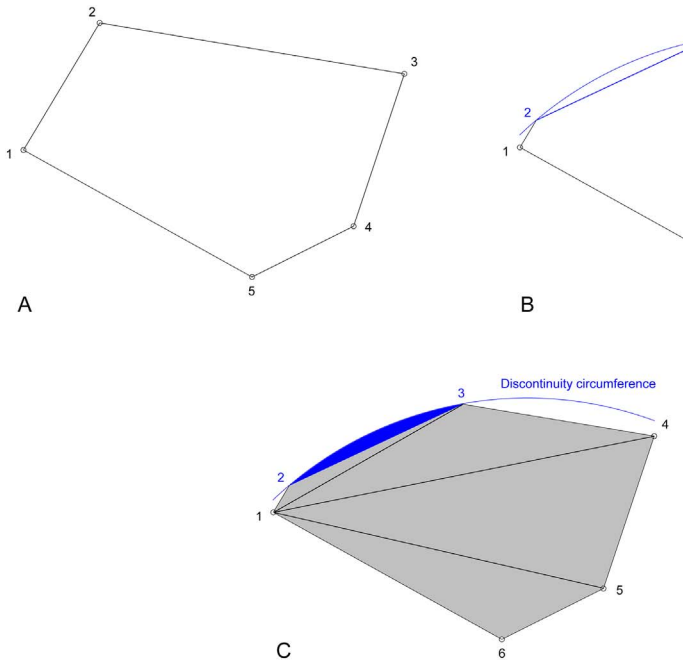

Fig. 1. A, Polygon representing the intersection between the discontinuity plane and a parallelepiped block. B, Replacement of the vertices located outside the discontinuity by the intersection points between the polygon and the discontinuity circumference. C, Calculation of the intersection area as the sum of triangle areas (gray) and circular segment areas (blue). (For interpretation of the references to color in this figure legend, the reader is referred to the web version of this article.)

value implies a more dispersed cluster. If κ is close to 0, the orientation of the discontinuity set is uniformly distributed.

2.2.2. Results

The results presented in Table 1 compare the statistics of the true discontinuity intensity P_{32} for the region under study with the average discontinuity intensity on borehole composite calculated by Eq. (1). It is notable that, at the scale of the entire region, there is little fluctuation in the true value of P_{32}, while at scale of the boreholes the variability in the average calculated P_{32} values is larger. In every case, there is no bias with regard to the true value, as the mean error is close to zero. These results corroborate that the experimental value $\hat{P}_{32}$ calculated with Eq. (1) is an unbiased estimator of the true value of P_{32}.

In Table 2 the same statistics are provided, but at the scale of sub-blocks with size 60 m × 60 m × 60 m. At this scale, one can observe that the fluctuation of the true value of P_{32} is moderate (up to ± 12% around the global average). In contrast, at the composite scale, fluctuations are considerable (larger in magnitude than in the sub-blocks), which means that, locally, there may be a significant deviation between the estimated and true values of P_{32}, although on average this deviation is zero. This can be explained because many small-size discontinuities have little chance to intersect the boreholes. In other words, the information contained in a single borehole represents a small fraction of the total information of the discontinuity network.

There are two alternatives to reduce the error (difference between the estimated and true values of P_{32}). The first one is to decrease the

Table 1
Statistics of true and experimental P_{32} for 500 simulations over a region with size 300 m × 300 m × 300 m.

Global discontinuity intensity (P_{32})	Number	Minimum (m^2/m^3)	Maximum (m^2/m^3)	Mean (m^2/m^3)	Standard deviation (m^2/m^3)
True	500	0.5938	0.6042	0.5990	0.0016
Experimental	500	0.5482	0.6908	0.6004	0.0222
Difference (error)	500	− 0.0923	0.0503	− 0.0014	0.0221

Table 2
Statistics of true and experimental P_{32} for 500 simulations over sub-blocks with size 60 m × 60 m × 60 m.

Local discontinuity intensity (P_{32})	Number	Minimum (m^2/m^3)	Maximum (m^2/m^3)	Mean (m^2/m^3)	Standard deviation (m^2/m^3)
True	62,500	0.5273	0.6685	0.5990	0.0169
Experimental	62,500	0.0851	10.007	0.6004	0.2279
Difference (error)	62,500	− 9.413	0.5280	− 0.0014	0.2272

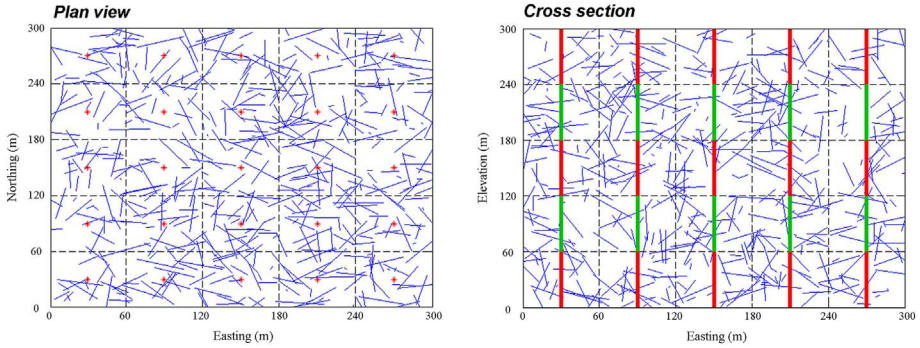

Fig. 2. Simulated DFN (blue solid lines) and sampling mesh (red stars) over a region with size 300 m × 300 m × 300 m (delimited with black solid lines) split into sub-blocks with size 60 m × 60 m × 60 m (delimited with black dashed lines). The composites on which the discontinuity intensity (P_{32}) is calculated are painted in red and green, alternately, along each vertical borehole. (For interpretation of the references to color in this figure legend, the reader is referred to the web version of this article.)

Table 3
Statistics of true and experimental P_{32} for 500 simulations over sub-blocks with size 60 m × 60 m × 300 m.

Local discontinuity intensity (P_{32})	Number	Minimum (m^2/m^3)	Maximum (m^2/m^3)	Mean (m^2/m^3)	Standard deviation (m^2/m^3)
True	12,500	0.5648	0.6270	0.5990	0.0077
Experimental	12,500	0.3657	2.3851	0.6004	0.1025
Difference (error)	12,500	− 1.7940	0.2237	− 0.0014	0.1022

borehole spacing and the second one is to increase the size of the sub-blocks on which the comparison is performed. Table 3 presents the calculated statistics based on the second alternative, by considering sub-blocks with size 60 m × 60 m × 300 m. It is notable that the standard deviation of the error is reduced by more than one half in comparison with the sub-blocks of 60 m high.

2.2.3. Discussion

According to the results of Tables 1, 2 and 3, the proposed methodology (Eq. (1)) gives an unbiased estimator of the discontinuity intensity P_{32}. It is based on the fact that P_{32} is a non-directional and additive variable, i.e., its value in a given block or region is the arithmetic average of the values in sub-blocks that form a regular partition of this block or region. These properties allow the use of the information defined on composites (borehole segments) to predict larger supports (blocks), without the need for inferring the distribution of the discontinuity parameters and for simulating the discontinuity networks in space.

In the presented synthetic case study, the distribution of discontinuities is homogeneous over space and a regular sampling with vertical drilling is considered. But the same methodology as the one described in Section 2.2.1 can be applied in more complex cases, for which the expected number of discontinuities and their diameters vary in space or for which the borehole sampling is performed unevenly.

3. Application to a real case study: El Teniente mine, Chile

In this section, the proposed methodology is applied to a real case study (El Teniente copper mine, Chile) to predict the discontinuity intensity and to estimate its uncertainty at unsampled locations. El Teniente, the largest copper-molybdenum deposit worldwide, is located in the Chilean Central Andes about 70 km south-southeast from Santiago, at latitude 34°05′16″S and longitude 70°23′15″W (Fig. 5). Its primary copper ore is currently mined by panel caving at a rate of about 140,000 tonnes per day (tpd). The rock types include hydrothermal breccias, as well as mafic (gabbros, diabases and CMET, a Spanish acronym for El Teniente Mafic Complex) and felsic (dacite and tonalite-diorite porphyries) intrusive rocks (Skewes et al., 2006).

Two main structure types are observed within the primary copper ore: a system of large-scale faults and a stockwork of small veins cemented with quartz, sulfides and anhydrite (Fig. 3) that define alteration zones according to their local abundance. It has been recognized that the rock mass disassembly during the caving propagation and fragmentation process occurs through veins with weaker infill mineral assemblages, named “weak veins”. These weak veins have a typical thickness greater than 1 mm and the percentage of their infill minerals logged as hard minerals is less than or equal to 35% (Fig. 4) (Brzovic and Villaescusa, 2007; Brzovic, 2009).

3.1. Data presentation and preparation

Two sources of core data, both located in the CMET rock type and collected by a team of geologists from El Teniente mine between 2010 and 2016, are available for this study. The first data set includes 75,569 logs, with information on the acute angle of the discontinuity (vein) with the borehole axis measured by geologists. The second data set (1975 logs) relates to oriented core techniques that allow identifying the dip and dip direction of the discontinuity plane, and not only its angle with the borehole axis. Henceforth, we only consider the weak veins (such that the proportion of hard minerals is less than or equal to 35%) with a typical thickness greater than or equal to 1 mm. Based on the lithological model of the study area (Fig. 5), the data sets are divided into two groups, named CMET-West and CMET-East. The motivation for this separation is the loss of spatial continuity that is expected for the intensity of weak veins when crossing the Dacite or Braden Breccia.

The next step is the calculation of the experimental P_{32} according to Eq. (1). Because of the variety of lengths analyzed along the boreholes (between 4 and 24 m in both data sets), a 1 m composite length is chosen in order to get as much detail as possible. Also, a minimum acute angle $\omega_i - \alpha$ of 15° is considered in Eq. (1) (i.e., the angle is increased to 15° when the original value is lower) to avoid dividing by a value close to zero. As a result of this step, one obtains two subsets of composite data with P_{32} values (CMET-West and CMET-East). Table 4 and Fig. 6 summarize the P_{32} statistics calculated in these subsets of data.

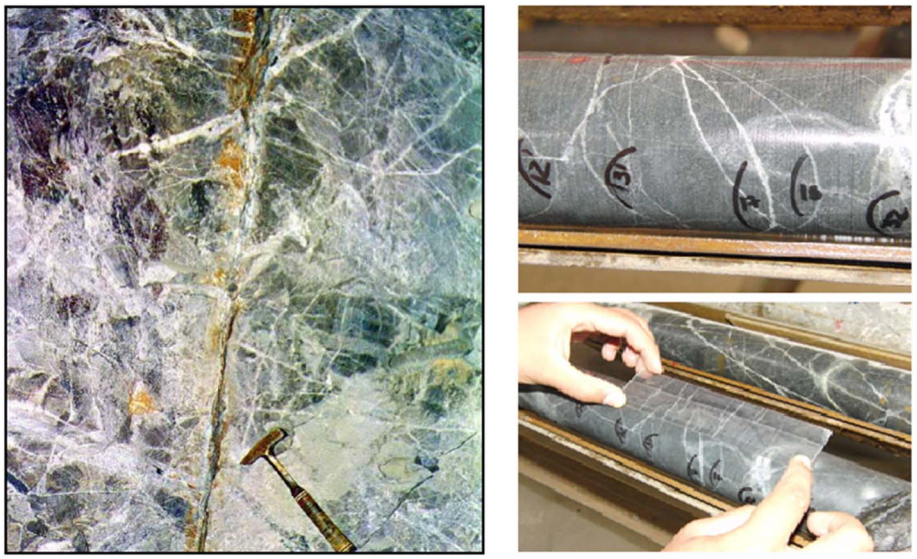

Fig. 3. Stockwork veins and faults recognized within the primary ore at a tunnel outcrop (left) and core data (right) at El Teniente mine (Brzovic and Villaescusa, 2007).

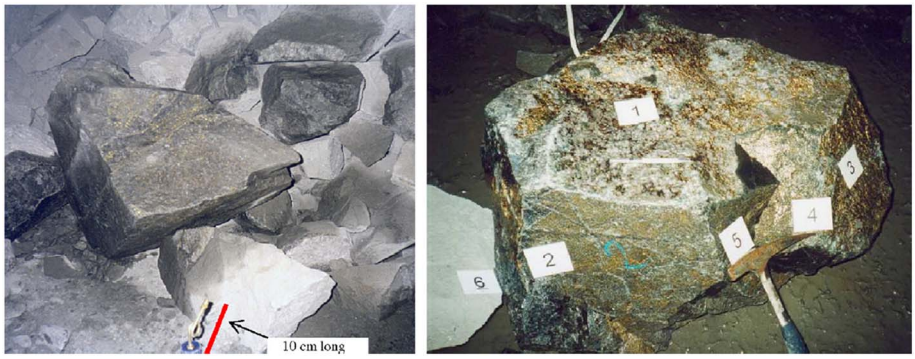

Fig. 4. Veins on faces of polyhedral caved rock blocks in draw points showing mineralogical infill such as chalcopyrite and quartz (Brzovic and Villaescusa, 2007).

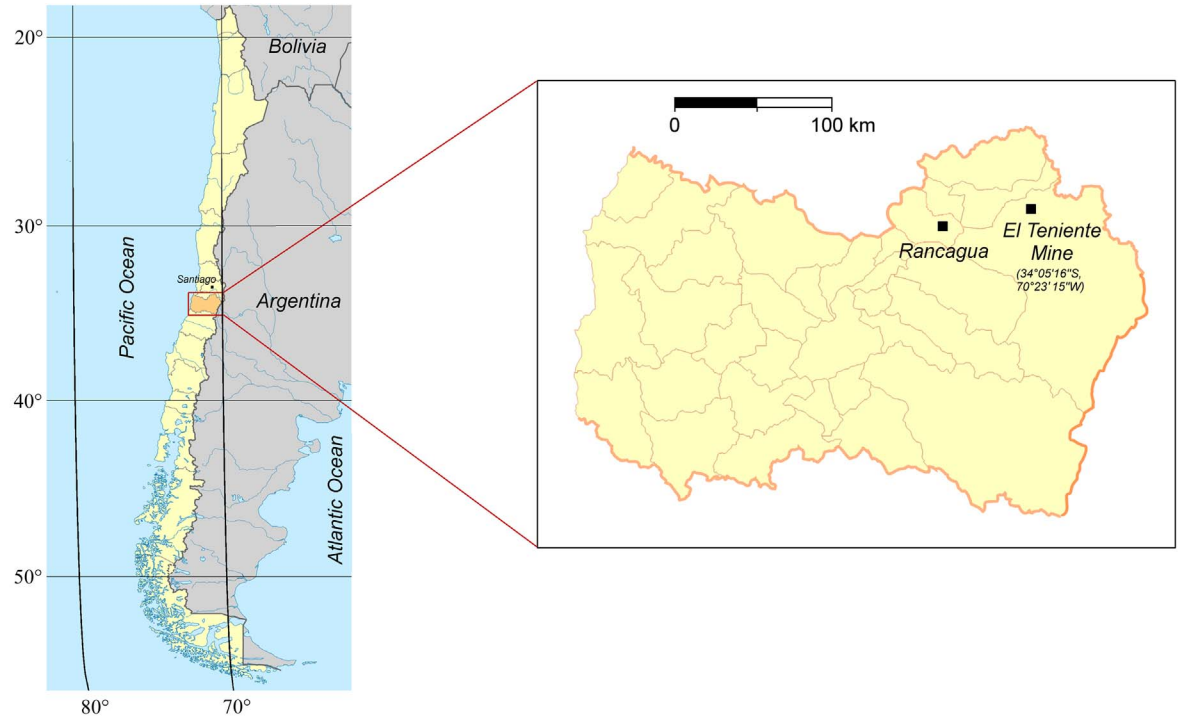

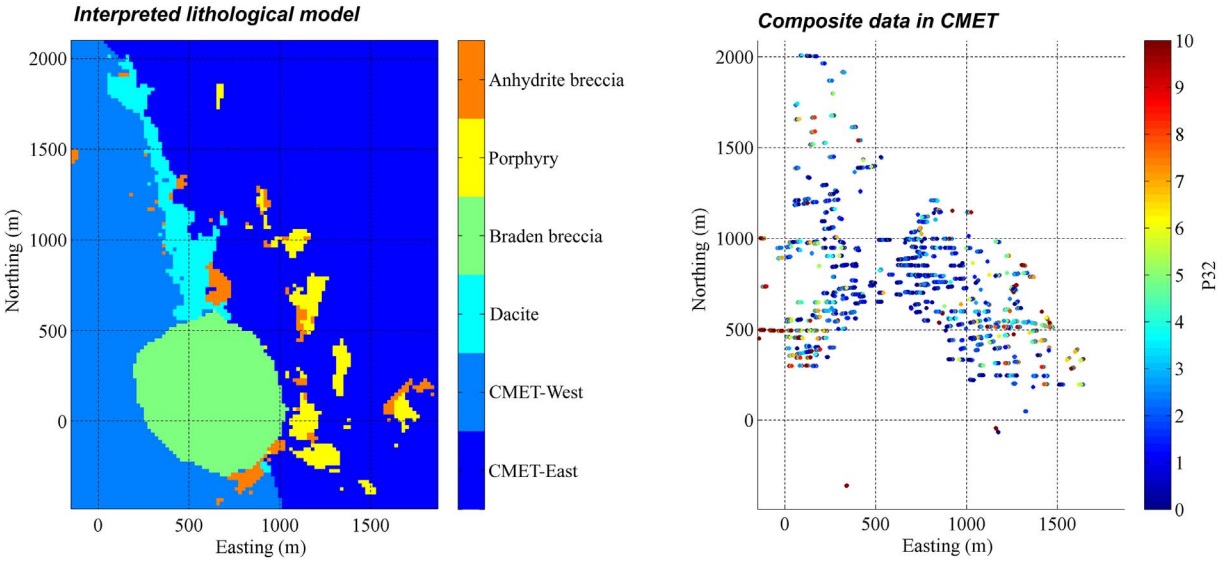

Fig. 5. Top: location of El Teniente mine (UTM coordinate system). Bottom: lithological model (elevation 2150 m) and location maps of borehole composites in CMET with elevations between 2100 and 2200 m, where the color indicates the experimental values of the weak vein intensity (local coordinate system).

Table 4
Basic statistics of the weak vein intensity (P_{32}) calculated in borehole composites.

	CMET East	CMET West
Number	29,743	13,485
Minimum (m^2/m^3)	0.00	0.00
Maximum (m^2/m^3)	49.46	52.54
Mean (m^2/m^3)	2.56	2.84
Standard deviation (m^2/m^3)	3.21	3.31

3.2. Simulating the intensity of weak veins

A spatial model of the weak vein intensity can be obtained by interpolating the values calculated in the borehole composites to blocks belonging to the CMET lithology. However, it is well-known (Chilès and Delfiner, 2012) that the interpolated values usually provide a smoothed map that does not reproduce the true spatial heterogeneity of the regionalized phenomenon. To avoid this smoothing effect, the formalism of geostatistical simulation can be used. It allows constructing a family of alternative outcomes (called realizations) whose spatial variability is similar to the reality, so that as many maps as desired reproducing the true heterogeneity at all spatial scales can be produced. A further step toward realism is to constraint the realizations to also reproduce the observed data. By generating several of these so-called conditional realizations, the spatial uncertainty can be quantified, e.g. via probability maps or probability intervals (Chilès and Delfiner, 2012).

In detail, to simulate the weak vein intensity, the Gaussian random field model is used, based on the following steps:

1) Apply cell declustering to the composite data, in order to remove the effect of sample clusters in both data sets (CMET-West and CMET-East).
2) Convert the P_{32} data into normal scores, i.e., data with a standard normal distribution. This transformation is performed in the CMET-West and CMET-East sectors separately.
3) Define a model of spatial correlation, via the calculation of an experimental variogram of the normal scores along the directions identified as principal directions of anisotropy (here, the horizontal plane and the vertical direction) and the fitting of a variogram model (Chilès and Delfiner, 2012). At this stage, a semi-automated fitting algorithm is used to minimize the mean squared error between the experimental and modeled variograms (Fig. 7). The variogram models in the CMET-West and CMET-East sectors consider a nugget effect and combinations of spherical models, as follows:

- Variogram model for intensity of weak veins in CMET-West:

$$\gamma_{West} = 0.51 \text{ nugget} + 0.11 \text{ sph}(5, 70) + 0.24 \text{ sph}(500, 1000) + 0.15 \text{ sph}(500, \infty) \quad (2)$$

- Variogram model for intensity of weak veins in CMET-East:

$$\gamma_{East} = 0.57 \text{ nugget} + 0.02 \text{ sph}(50, 50) + 0.10 \text{ sph}(500, 50) + 0.23 \text{ sph}(600, \infty) \quad (3)$$

In Eqs. (2) and (3), the values into parentheses indicate the correlation ranges (in meters) along the horizontal and vertical directions, respectively, whereas the coefficient before each basic spherical structure (sph) indicates the partial sill associated with this structure. Note that more than one half of the total sill corresponds to a nugget effect, which indicates that the weak vein intensity calculated on the composite support has predominant short-scale variability.

4) Simulate Gaussian random fields in the CMET-West and CMET-East sectors, conditioned to the composite data (i.e., restricting the realizations to reproduce the normal scores values at the composites locations). The simulation is done with a spectral-turning bands algorithm (Emery et al., 2016) and the conditioning is done by post-processing the realizations with ordinary kriging (Chilès and Delfiner, 2012). A total of 500 realizations are constructed on a fine grid with a mesh size of 4 m × 4 m × 10 m, which are then back-transformed from the Gaussian scale to the P_{32} scale and averaged onto block with a size of 20 m × 20 m × 20 m. Table 5 indicates the main implementation parameters used for turning bands simulation.

3.3. Post-processing the realizations

Fig. 8 shows a plan view of the minimum, average and maximum simulated weak vein intensity in each block for elevation 2150 m; only the CMET blocks distant less than 100 m from a borehole have been considered for simulation (the interpolation at more distant blocks is deemed unreliable by the geologists of El Teniente mine, for lack of nearby conditioning data). The minimum and maximum simulated values deliver, block by block, a bounded interval that should contain the real value of the weak vein intensity with a confidence level close to 1. Actually, for a given block, the probability that the actual P_{32} value is less than the minimum of 500 realizations or greater than the maximum of 500 realizations is 1/501, therefore the probability that it is between the minimum and the maximum is 499/501 = 99.6%. An interval associated with any other confidence level $p \in [0,1]$ can also be derived by considering the $(1 - p)/2$ and $(1 + p)/2$ quantiles of the

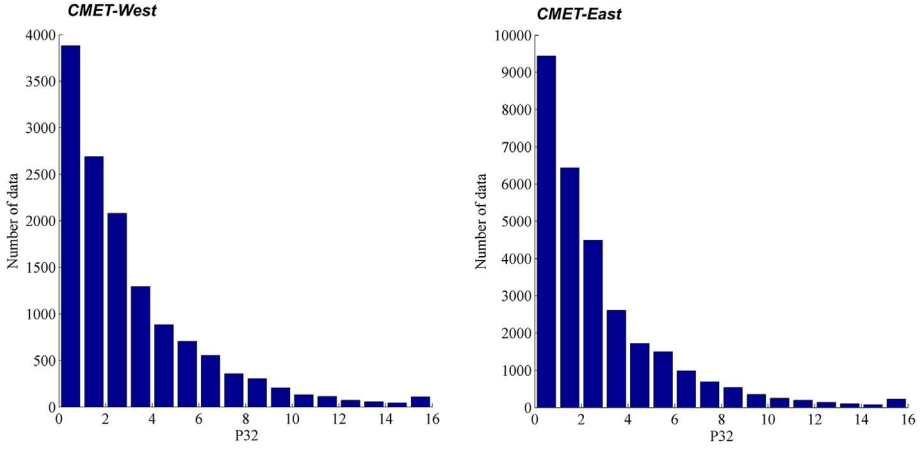

Fig. 6. Experimental distribution of weak vein intensity in borehole composites. Left: CMET-west sector. Right: CMET-East sector.

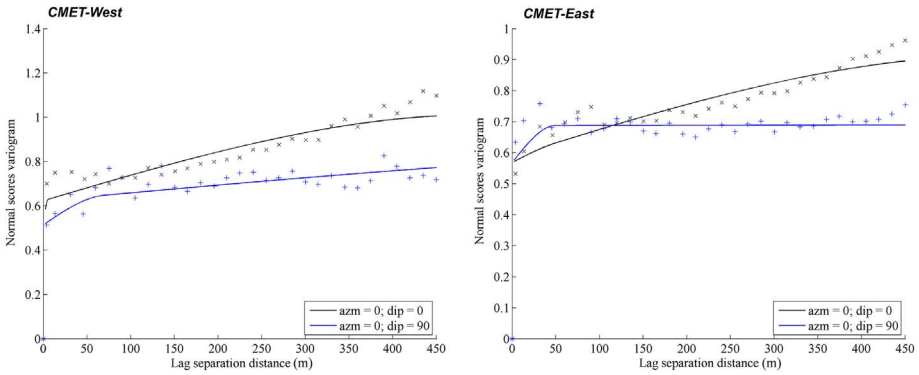

Fig. 7. Experimental (crosses) and modeled (lines) variograms along the main directions of anisotropy for the normal scores of weak vein intensity, in CMET-West (left) and CMET-East (right).

Table 5
Parameters for spectral-turning bands simulation.

Parameter	Value
Radius for searching conditioning data	800 m
Optimal number of data per octant	150
Number of realizations	500
Number of turning lines	1000

distribution of simulated P_{32} values as the lower and upper bounds, respectively.

In Fig. 9, the first realization of weak vein intensity at elevation 2150 m is displayed. This map exhibits a greater variability in comparison with the average of 500 realizations (Fig. 8), which shows a smoothed version of the intensity spatial distribution. In contrast, each realization reproduces the true variability at all spatial scales, even if the simulated values within the blocks of 20 × 20 m × 20 m exhibit less variability than the composite data due to the support effect when passing from the (small) volume of a 1 m-length composite to the (larger) volume of a block (Chilès and Delfiner, 2012).

The realizations can also be used to map the probability that the true (unknown) weak vein intensity is greater than a pre-specified threshold, identified as the frequency with which the simulated values exceed such a threshold. As an illustration, Fig. 10 shows the probability maps associated with thresholds 5 and 7 for a given elevation (2150 m). The calculated probability depends not only on the expected value of the weak vein intensity, but also on the dispersion around the

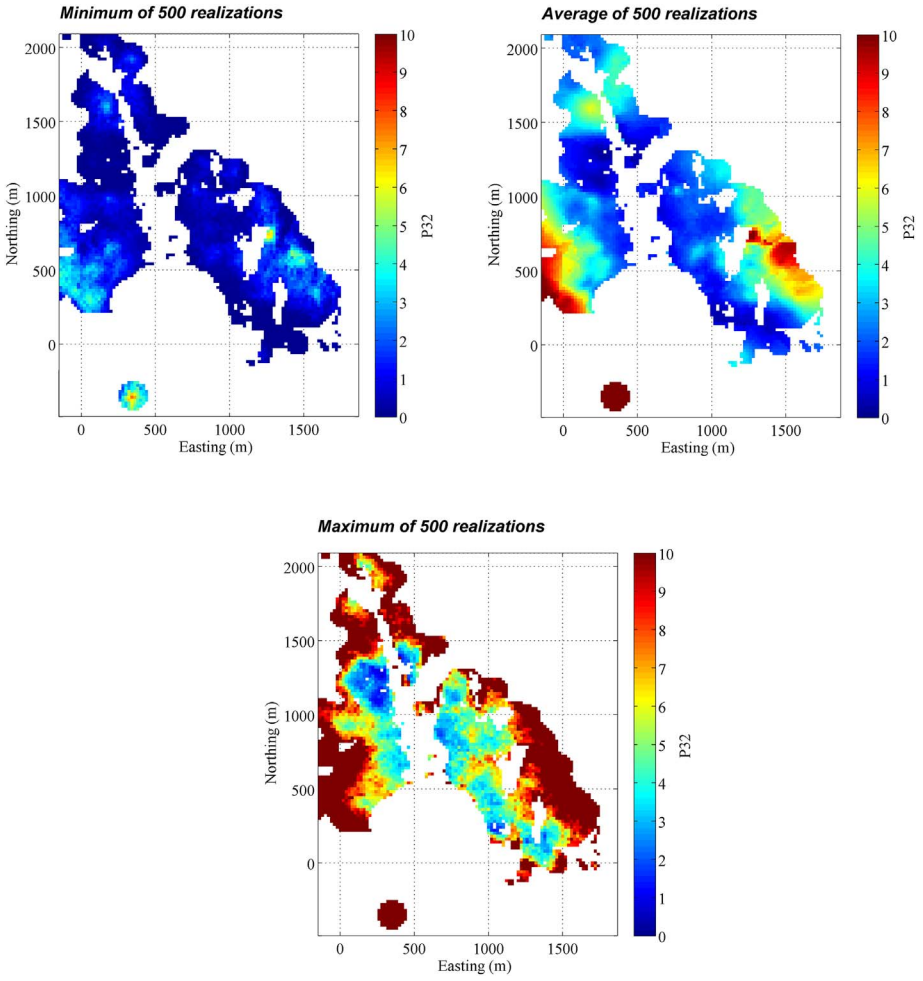

Fig. 8. Plan view of minimum, average and maximum simulated weak vein intensity in CMET lithology for elevation 2150 m, calculated from 500 realizations.

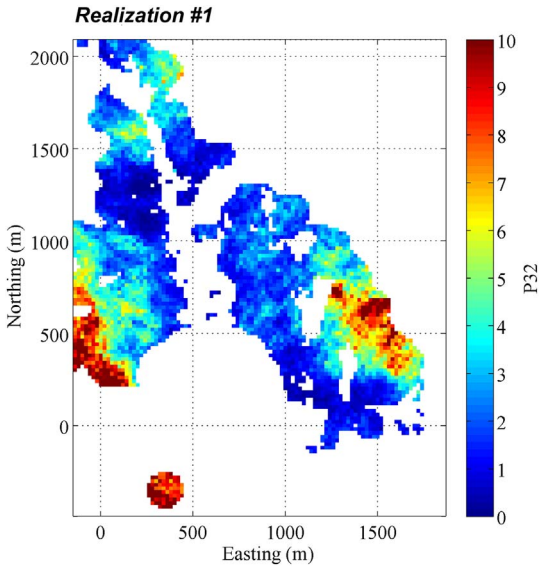

Fig. 9. Map of the simulated weak vein intensity in CMET lithology at elevation 2150 m (first realization).

expected value (a high dispersion may imply that there is a significant risk of finding a high P_{32} value, even if the average over the realizations is lower than the threshold). The probability maps can be further used to divide the region under study, for example into a low damage zone, an intermediate damage zone and a high damage zone, with respect to given critical P_{32} values and levels of uncertainty that are defined by the practitioner according to his/her expert knowledge.

3.4. Model validation

Leave-one-out cross-validation is a technique aimed at verifying the quality of spatial prediction and uncertainty models, by testing these models with available borehole composite data. This technique consists in: (1) removing one composite data from the database, (2) simulating the weak vein intensity value at the coordinates of the removed data based on all the other available data, (3) repeating steps (1) and (2) for each composite data, and (4) comparing the actual intensity values with the simulated values.

Regarding step (2), let us consider the same algorithm (spectral-turning bands) and the same input parameters (variogram models, moving neighborhood to search the conditioning data, type of kriging for conditioning the realizations, number of turning lines and number of realizations) as those used to construct the former block models, except for the block discretization that does not apply in this case, as the simulation is performed at the data composite support.

With regard to step (4), two types of validations are contemplated:

1) Validation of the prediction ability of simulation. A prediction of the weak vein intensity can be obtained by averaging all the realizations. Then, this prediction can be compared with the actual values, using a dispersion cloud where the real value is placed in ordinate and the predicted value in abscissa. It is intended that the points of the cloud are scattered around the diagonal line with a regression line with an intercept close to zero and a slope close to one, in which case the prediction has no bias or conditional bias (Chilès and Delfiner, 2012).
2) Validation of the ability to measure uncertainty. In this case, it is intended to check whether or not the set of realizations properly quantifies the uncertainty in the actual values of the weak vein intensity. To this end, from the simulated values at each data location, one can define an interval where the real value has some probability p to be. Then, the probability p is compared to the proportion p^* of data whose actual values are effectively within their respective intervals, through a curve that will be called “uncertainty graph”. Ideally, the uncertainty graph should match the diagonal line, indicating that the theoretical probabilities calculated from the realizations coincide with the statistical proportion of true values that belong to the probability intervals.

Figs. 11 and 12 show the results obtained in the CMET-West and CMET-East sectors. In all cases, an excellent predictability (linear regressions close to the diagonal line) and capability of measuring uncertainty (uncertainty graphs close to the diagonal line) are observed, which validates the models constructed in the former subsection.

4. Discussion and conclusions

The proposed methodology allows the direct calculation of the discontinuity intensity in borehole composites, without the need for modeling the distributions of the discontinuity centers, sizes and orientations, by weighting each discontinuity intersecting a borehole by the inverse of the cosine of the acute angle between the borehole direction and the direction normal to the discontinuity plane. This weighting is consistent with the Terzaghi correction, implying that the discontinuities oblique to the borehole take more weight in comparison with discontinuities that are orthogonal to it. The only practical restriction for calculating the composite data corresponds to the definition of a minimum angle (15° in this work) to avoid extremely large weights for discontinuities sub-parallel to the boreholes.

Provided that there are enough data available for variogram analysis, the proposed approach is more straightforward than other available approaches of Zhang and Einstein (2000), based on combining estimates

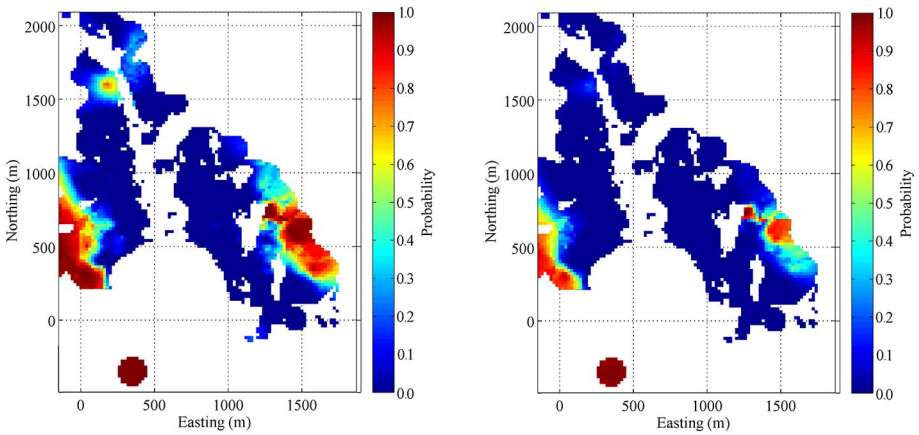

Fig. 10. Maps of the probability that the actual weak vein intensity is greater than 5 (left) or 7 (right) at elevation 2150 m.

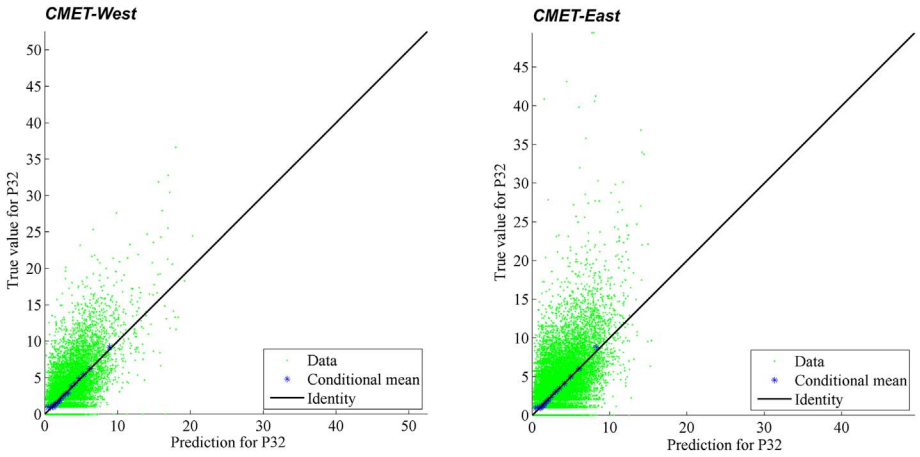

Fig. 11. Scatter plots between actual and predicted values (average of 500 realizations) in the CMET-West (left) and CMET-East (right) sectors. The abscissa axis has been split into 20 intervals and the gravity centers of the points located within each interval are plotted as an approximation of the conditional mean curve.

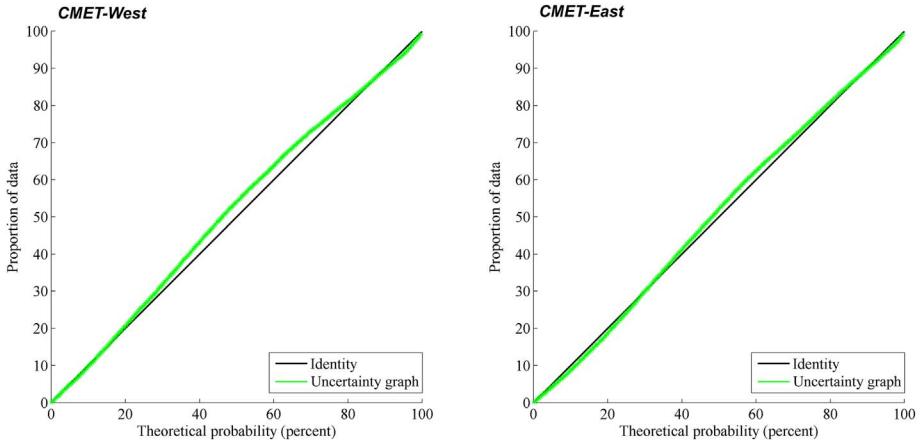

Fig. 12. Uncertainty graphs in the CMET-West (left) and CMET-East (right) sectors.

of the size distribution and the number of discontinuities, or of Dershowitz and Herda (1992), based on calculating a conversion factor between the discontinuity intensity (P_{32}) and the discontinuity frequency (P_{10} or P_{21}). The latter two approaches rely on parameters (in particular, the discontinuity frequency and the factor converting it into P_{32}) that depend on the direction on which they are measured, do not average linearly (non-additivity) and may be poorly estimated. All these drawbacks are avoided by working directly with the discontinuity intensity P_{32}. Since P_{32} is an additive variable (its value in a given volume is defined as the average of the values at the points that make up this volume) and non-directional, block models of this variable can be built directly from the borehole composite data, via spatial interpolation techniques. Also, conditional simulation techniques can be used to map the spatial variability of the intensity of discontinuities and to quantify the uncertainty in the value of each block, by defining confidence limits.

With respect to the real case study (El Teniente mine), the discontinuity intensity exhibits an erratic behavior on the composite support, with a significant fraction of the spatial continuity modeled by a nugget effect. However, a spatial correlation with a considerable range (several hundreds of meters) is observable, which proves that the discontinuity intensity is regionalized. By selecting a 20 m × 20 m × 20 m block support, the nugget effect is no longer perceptible and the constructed models essentially represent the spatially continuous component. In the realizations obtained by simulation, sectors of low discontinuity intensity values are adjacent to the Dacite body, while the sectors of high values are in the extreme east and west of the region of interest and are completely distinguishable from other areas. Another sector with a high discontinuity intensity value is located in the southwest of the Braden Breccia, but this sector is characterized by few boreholes.

As a future work, the feasibility of incorporating additional data to improve the predicted values and to reduce the uncertainty in the discontinuity intensity will be investigated, for example by using gallery mapping data and/or geochemical data (copper grade assays) that may be correlated with the discontinuity intensity.

Acknowledgments

This research was supported by the Chilean Commission for Scientific and Technological Research, through Project CONICYT/FONDECYT/REGULAR/N°1170101. The authors are grateful to the anonymous reviewers for their comments on previous versions of this manuscript, to Karen Baraona, Violeta Ríos, Sebastián González, María Paz Sepulveda and Iván Rojas from Codelco-El Teniente for providing the data used in the case study, and to Codelco Chile for authorizing the publication of this work.

References

Brzovic, A., 2009. Rock mass strength and seismicity during caving propagation at the El Teniente Mine, Chile. In: Tan, C.A. (Ed.), 7th International Symposium on Rockburst and Seismicity in Mines (RaSiM7). Rinton Press, New York, pp. 838–852.

Brzovic, A., Villaescusa, E., 2007. Rock mass characterization and assessment of block-forming geological discontinuities during caving of primary copper ore at the El Teniente mine, Chile. Int. J. Rock Mech. Min. Sci. Geomech. Abstr. 44, 565–583.

Chilès, J.P., Delfiner, P., 2012. Geostatistics: Modeling Spatial Uncertainty, second ed. Wiley, New York.

Chilès, J.P., Wackernagel, H., Beucher, H., Lantuéjoul, C., Elion, P., 2008. Estimating fracture density from a linear or areal survey. In: Ortiz, J.M., Emery, X. (Eds.), Proceedings of the Eighth International Geostatistics Congress. Gecamin Ltda, Santiago, pp. 535–544.

Dershowitz, W.S., Herda, H.H., 1992. Interpretation of fracture spacing and intensity. In: Tillerson, J.R., Wawersik, W.R. (Eds.), Proceedings of the 33th U.S. Symposium on

Rock Mechanics. A.A. Balkema, Rotterdam, pp. 757–766.
Emery, X., Arroyo, D., Porcu, E., 2016. An improved spectral turning-bands algorithm for simulating stationary vector Gaussian random fields. Stoch. Env. Res. Risk A. 30 (7), 1863–1873.
Fisher, R., 1953. Dispersion on a sphere. Proc. R. Soc. Lond. A Math. Phys. Sci. 217 (1130), 295–305.
Gonzalez, R., Brzovic, A., 2015. Características de las fallas con potencial de generar estallidos de rocas, en mina El Teniente (Characteristics of faults susceptible to generate rock bursts in El Teniente Mine). In: Aracena, I., Freire, R., Ibarra, F., Menzies, A. (Eds.), Proceedings of the Fourth International Seminar on Geology for the Mining Industry. Gecamin Ltda, Santiago.
Riquelme, A.J., Abellán, A., Tomás, R., 2015. Discontinuity spacing analysis in rock masses using 3D point clouds. Eng. Geol. 195, 185–195.
Skewes, M.A., Arevalo, A., Floody, R., Zuniga, P., Stern, C.R., 2006. The El Teniente megabreccia deposit, the world's largest deposit. In: Porter, T.M. (Ed.), Super Porphyry Copper and Gold Deposits - A Global Perspective. Porter Geoscience Consultancy Publishing, Adelaide, Australia, pp. 83–113.
Sturzenegger, M., Stead, D., Elmo, D., 2011. Terrestrial remote-sensing-based estimation of mean trace length, trace intensity and block size/shape. Eng. Geol. 119 (3–4), 96–111.
Terzaghi, R.D., 1965. Sources of error in joint surveys. Geotechnique 15 (3), 287–303.
Tuckey, Z., Stead, D., 2016. Improvements to field and remote sensing methods for mapping discontinuity persistence and intact rock bridges in rock slopes. Eng. Geol. 208, 136–153.
Yow Jr., J.L., 1987. Blind zones in the acquisition of discontinuity orientation data. Int. J. Rock Mech. Min. Sci. Geomech. Abstr. 24 (5), 317–318.
Zhang, L., Einstein, H.H., 2000. Estimating the intensity of rock discontinuities. Int. J. Rock Mech. Min. Sci. 37, 819–837.